Journal of Medical Systems (2019) 43: 285
https://doi.org/10.1007/s10916-019-1415-1

IMAGE & SIGNAL PROCESSING

An Automatic Approach Using ELM Classifier for HFpEF Identification Based on Heart Sound Characteristics

Yongmin Liu[1] · Xingming Guo[1] · Yineng Zheng[2]

Received: 8 May 2019 / Accepted: 3 July 2019 / Published online: 15 July 2019

Abstract

Heart failure with preserved ejection fraction (HFpEF) is a complex and heterogeneous clinical syndrome. For the purpose of assisting HFpEF diagnosis, a non-invasive method using extreme learning machine and heart sound (HS) characteristics was provided in this paper. Firstly, the improved wavelet denoising method was used for signal preprocessing. Then, the logistic regression based hidden semi-Markov model algorithm was utilized to locate the boundary of the first HS and the second HS, therefore, the ratio of diastolic to systolic duration can be calculated. Eleven features were extracted based on multifractal detrended fluctuation analysis to analyze the differences of multifractal behavior of HS between healthy people and HFpEF patients. Afterwards, the statistical analysis was implemented on the extracted HS characteristics to generate the diagnostic feature set. Finally, the extreme learning machine was applied for HFpEF identification by the comparison of performances with support vector machine. The result shows an accuracy of 96.32%, a sensitivity of 95.48% and a specificity of 97.10%, which demonstrates the effectiveness of HS for HFpEF diagnosis.

Keywords Heart failure with preserved ejection fraction · Heart sounds · Multifractal detrended fluctuation analysis · Extreme learning machine

Introduction

Heart failure with preserved ejection fraction (HFpEF) accounts for approximately 50% of all heart failure (HF) patients [1], and it is often associated with multiple comorbidities, including hypertension, obesity, atrial fibrillation and metabolic syndrome [2]. In addition, the morbidity and mortality of HFpEF are comparable to or a little lower than HF with reduced ejection fraction [1, 3], but the diagnosis of HFpEF is more challenging [4].

The following conditions should be considered for HFpEF diagnosis according to the 2016 European Society of Cardiology Guidelines [4]: (1) The symptoms and/or signs of HF. (2) A preserved left ventricular ejection fraction (≥ 50%). (3) An increased B-type natriuretic peptide (BNP > 35 pg/ml) and/or N-terminal pro-BNP (> 125 pg/ml). (4) Evidence of other changes in cardiac structure or function. (5) An elevated left ventricular filling pressure confirmed by stress test or invasive measurement. However, many HFpEF patients show symptoms only after exercise and the BNP will not elevate when such individuals are in rest state [5]. Moreover, the symptoms and signs of HFpEF patients are non-specific for HFpEF is the early stage of HF, and the invasive measurement is not suitable to promote among people. All of these may lead guideline based HFpEF diagnosis to be insensitive. Hence, it is of great significance to explore new directions for HFpEF diagnosis. Tells et al. [6] found that novel cardiovascular imaging modalities seems promising for HFpEF characterization. Heart sound (HS) can provide effective information for early recognition of cardiac abnormalities due to its direct reflection of the mechanical properties of cardiac activity [7]. However, to the best of our knowledge, the study of HFpEF using HS has not been reported yet.

This article is part of the Topical Collection on *Image & Signal Processing*

✉ Xingming Guo
guoxm@cqu.edu.cn

[1] Key Laboratory of Biorheology Science and Technology, Ministry of Education, College of Bioengineering, Chongqing University, Chongqing 400044, China

[2] Department of Radiology, the First Affiliated Hospital of Chongqing Medical University, Chongqing 400016, China

HS is a non-stationary physiological signal with obvious multifractal characteristics [8]. Multifractal detrended fluctuation analysis (MF-DFA) [9] is regarded as an effective method for analyzing the multifractality of non-stationary signals. Zheng et al. [10] manifest that normal HS has a stronger multifractality than HF based on MF-DFA. Sikdar et al. [11] used MF-DFA for electroencephalogram classification and obtained a high accuracy of 99.6%. Besides, Lin and Chen [12] utilized MF-DFA to detect the fault gear. Tang et al. [13] applied MF-DFA method for partial discharge signals analysis. The aforementioned studies demonstrate the effectiveness of MF-DFA in dealing with complex and non-stationary nonlinear signals, however, the research on HS using MF-DFA method has been rarely reported yet.

In previous study, the support vector machine (SVM) with gaussian radial basis kernel function was confirmed to have a good performance in HS classification [14], but the values of kernel function parameter δ and penalty parameter C are difficult to select appropriately. Many intelligent optimization algorithms such as particle swarm optimization [15], ant colony optimization [16] and social emotional optimization [17] were proposed for parameters optimization, but it will take a long time. Extreme learning machine (ELM) is an extremely effective method [18], which achieves similar or preferable generalization performance at much faster speed than SVM [19].

Therefore, we proposed an automatic approach using ELM classifier for HFpEF identification based on HS characteristics in this study. The preprocessing was implemented based on resampling, modified wavelet denoising and amplitude normalization. The ratio of diastolic to systolic duration (D/S) and 11 MF-DFA based features were calculated by means of average method and MF-DFA, respectively. Then a t-test was performed on the above characteristics, the features with significant differences were selected to generate the diagnostic feature set, which was input into ELM for HFpEF identification, and SVM was designed for comparison in order to testify the superiority of the proposed method.

The remaining of this paper is structured as follows. In "Materials and methods" section, the experimental data as well as the algorithms of preprocessing, features extraction and classification are introduced. The "Results" section describes the statistical results of the extracted HS characteristics and compares the performance of ELM and SVM. In "Discussion" section, the differences of the features between healthy people and HFpEF patients are discussed, moreover, the advantages and limitations of this study are analyzed. The "Conclusion" section summarizes the preliminary conclusions and puts forward some suggestions for future work.

Materials and methods

Selection and description of data

The dataset selected for this study consists of 401 HS signals from healthy volunteers with no history of cardiovascular disease in Chongqing University as control group, and 441 HS signals from HFpEF patients who were diagnosed and confirmed by the cardiologists in University-Town Hospital of Chongqing Medical University as experimental group. All the data were acquired by the HS collector (Patent No: CN2013093000306700) at the sampling frequency of 11025 Hz when the subjects are in rest state.

Data preprocessing

Since the frequency of HS generally does not exceed 800 Hz [20], firstly, the signals were resampled into 2205 Hz according to the Nyquist sampling theorem. Then, the improved wavelet denoising method where the different mother wavelet as well as decomposition layer for different signals were selected adaptively based on the method described in article [21], the threshold values at different decomposition level and the threshold function were calculated based on Eq. (1) [22] and Eq. (2) [23], respectively.

$$\lambda_j = \frac{\sigma\sqrt{2\ln N}}{\ln(e+j-1)},\quad j = 1, 2, \ldots J \tag{1}$$

$$D_j^T[k] = \begin{cases} D_j[k] & , \quad if\,|D_j[k]| > \lambda_j \\ D_j[k]^3/{\lambda_j}^2 & , \quad if\,|D_j[k]| \le \lambda_j \end{cases} \tag{2}$$

where N is the length of the signal, J represents the total number of decomposition layer, e is the natural logarithm, D_j is the detail coefficient of jth decomposition level, let MAD represents the median of absolute value, $\sigma = MAD\{D_j[k]\}/0.6745$ denotes the standard deviation of noise [24]. Finally, the amplitude normalization was applied to the denoised signal $S(n)$:

$$S_{norm}(n) = \frac{S(n)}{\max_{n=1}^{N}(|S(n)|)} \tag{3}$$

HS characteristics extraction

The D/S

The D/S value (illustrated in Fig. 1) is a time index that has the ability to assess whether the blood perfusion time of myocardial is sufficient during diastole [25]. It can be used as a non-invasive indicator for cardiac function assessment of HFpEF patients. Firstly, the signals were segmented by the logistic regression based hidden semi-Markov model [26–28], then,

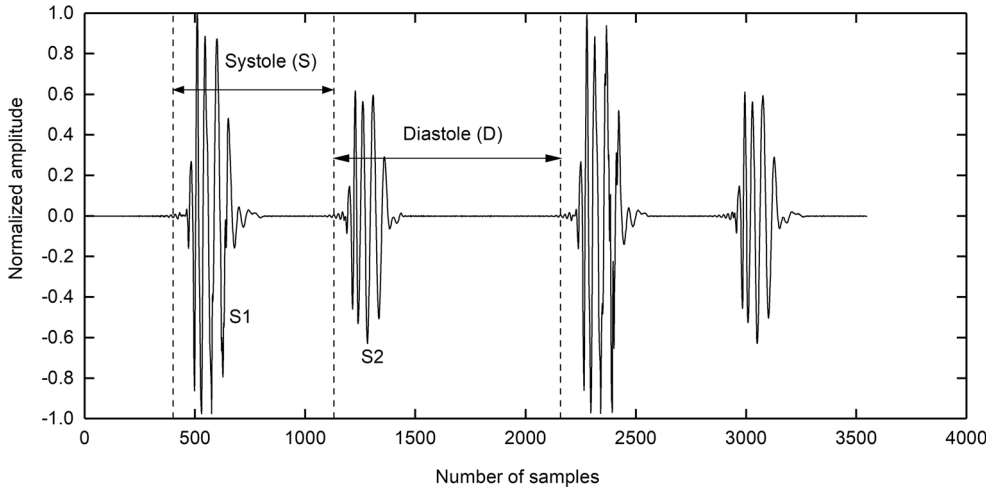

Fig. 1 The illustration of the ratio of diastolic to systolic duration

calculated the average value of D/S over 20 cycles as the result.

MF-DFA based features

Generally, multifractal characteristics of time series can be divided into two types, one is because of the broad probability density function, and the other is because of the different long-range correlations of large and small fluctuations [29]. The MF-DFA method, which enables both integral and local detection of the multifractality, was utilized to analyze the multifractal characteristics of HS in this study. Supposing that $\{x_k\}$ is a compact support discrete time series of length N, the algorithms of MF-DFA [9] are as follows:

Step 1: Calculate the "profile":

$$Y(i) = \sum_{k=1}^{i} \left[x_k - \bar{x}\right], \quad i = 1, 2, ..., N \tag{4}$$

where $\bar{x}$ denotes the average value of x_k.

Step 2: Divide $Y(i)$ into $N_s = \text{int}[N/s]$ non-overlapping segments of length s and repeat this procedure from opposite end to avoid data disregarding. The length of minimum segments should be large to avoid overfitting, while the length of maximum segments should be small to provide adequate segments for fluctuation function calculation [30], which were set as 28 and $N/10$, respectively.

Step 3: For each segment, the least-square fit using second order polynomial was selected to calculate the local trend $y_v(i)$, and the fluctuations $F^2(s, v)$ are calculated as:

$$F^2(s,v) = \frac{1}{s} \sum_{i=1}^{s} \{Y[(v-1)s + i] - y_v(i)\}^2, \quad v = 1, 2, ..., N_s \tag{5}$$

$$F^2(s,v) = \frac{1}{s} \sum_{i=1}^{s} \{Y[N-(v-N_s)s + i] - y_v(i)\}^2, \quad v = N_s + 1, N_s + 2, ..., 2N_s \tag{6}$$

where s is the segment size, $v \in [1, 2N_s]$ is the current segment number.

Step 4: The q order fluctuation function is:

$$F_q(s) = \left\{ \frac{1}{2N_s} \sum_{v=1}^{2Ns} \left[F^2(s,v)\right]^{\frac{q}{2}} \right\}^{\frac{1}{q}} \tag{7}$$

where q is the weight of local fluctuations and can be any non-zero real values, $q > 0$ represents the large fluctuations and $q < 0$ represents the small fluctuations [30], when $q = 0$, the fluctuation function can be obtained based on Eq. (8). In addition, the calculation accuracy will decrease with the increase of $|q|$ [30]. A choice of q between −3 and 3 is sufficient in this paper.

$$F_0(s) = \exp\left\{ \frac{1}{4N_s} \sum_{v=1}^{2N_s} \ln\left[F^2(s,v)\right] \right\} \tag{8}$$

If the signal is long-range power-law dependent, the relationship between $F_q(s)$ and s can be written as:

$$F_q(s) \propto s^{h(q)} \tag{9}$$

where $h(q)$ is the slope of log-log plot of $F_q(s)$ versus s, which is called the generalized Hurst exponent, and it is directly related to the scaling exponent $\tau(q)$ in standard multifractal analysis.

$$\tau(q) = qh(q) - 1 \tag{10}$$

Applying the Legendre transform to $\tau(q)$, the singularity exponent α and its corresponding dimension $f(\alpha)$ can be obtained as follows:

$$\alpha = h(q) + qh'(q) \tag{11}$$

$$f(\alpha) = q[\alpha - h(q)] + 1 \tag{12}$$

Eleven features were calculated based on MF-DFA with the full use of $h(q)$, $\tau(q)$, α and $f(\alpha)$ in this study, and the detailed interpretations of these parameters are shown in Table 1.

ELM-based classification

An ELM is a single hidden layer feedforward network (shown in Fig. 2) with the parameters of hidden neurons selected stochastically and the output weights determined directly without iteration. For datasets $\{x_j, t_j\}$, $j = 1, ..., N$, where $x_j = [x_{j1}, x_{j2}, ..., x_{jn}]^T \in R^n$ represents the input features, $t_j = [t_{j1}, t_{j2}, ..., t_{jm}]^T \in R^m$ denotes the labels of x_j, N is the number of samples selected in this study. The structure of ELM with L hidden neurons can be represented as [18]:

$$\sum_{i=1}^{L} \beta_i g(w_i \cdot x_j + b_i) = o_j, \quad j = 1, ..., N \tag{13}$$

where $w_i = [w_{i1}, w_{i2}, ..., w_{in}]^T$ and $\beta_i = [\beta_{i1}, \beta_{i2}, ..., \beta_{im}]^T$ are the weight vectors connecting the *ith* hidden neuron with the input neurons and the output neurons, respectively. b_i represents the threshold of the *ith* hidden neuron. $w_i \cdot x_j$ denotes the inner product of w_i and x_j, $g(x)$ is the activation function, o_j is the output of the network corresponding to the input x_j. This model can approximate all the input samples without deviation, which means:

$$\sum_{j=1}^{N} \|o_j - t_j\| = 0 \tag{14}$$

$$\sum_{i=1}^{L} \beta_i g(w_i \cdot x_j + b_i) = t_j, \quad j = 1, ..., N \tag{15}$$

Table 1 The definitions of the extracted MF-DFA based features in this study

Symbol	Definition
H	Hurst exponent, the value of $h(q)$ when $q = 2$
$h(q_{min})$, $h(q_{max})$	The value of $h(q)$ when q takes the minimum or maximum value
$\tau(q_{min})$, $\tau(q_{max})$	The value of $\tau(q)$ when q takes the minimum or maximum value
α_{max}, α_{min}	The maximum or minimum value of α
$\Delta\alpha$	Multifractal spectrum width, where $\Delta\alpha = \alpha_{max} - \alpha_{min}$
$f(\alpha_{max})$, $f(\alpha_{min})$	The fractal dimension corresponding to α_{max} or α_{min}
Δf	$\Delta f = f(\alpha_{max}) - f(\alpha_{min})$

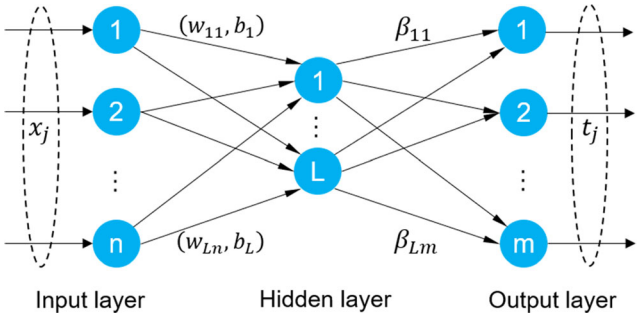

Fig. 2 The network of extreme learning machine

The Eq. (15) can be rewritten as $H_L\beta = T$, where

$$H_L(w_1, ..., w_L, b_1, ..., b_L, x_1, ..., x_N) = \begin{bmatrix} g(w_1x_1 + b_1) & ... & g(w_Lx_1 + b_L) \\ ... & ... & ... \\ g(w_1x_N + b_1) & ... & g(w_Lx_N + b_L) \end{bmatrix}_{N \times L} \tag{16}$$

$$\beta = \begin{bmatrix} \beta^T{}_1 \\ ... \\ \beta^T{}_L \end{bmatrix}_{L \times m}, T = \begin{bmatrix} t^T{}_1 \\ ... \\ t^T{}_N \end{bmatrix}_{N \times m} \tag{17}$$

where H_L is called the output matrix of hidden layer.

Once w_i and b_i are randomly determined, H_L is uniquely defined correspondingly. Therefore, β can be obtained by:

$$\hat{\beta} = H_L{}^{\dagger} T \tag{18}$$

where $H_L{}^{\dagger}$ denotes the Moore-Penrose generalized inverse of H_L. Thereby, the output of ELM is as follows:

$$f(x_j) = \sum_{i=1}^{L} \hat{\beta}_i g_i(w_i \cdot x_j + b_i) \tag{19}$$

Results

The statistical results of HS characteristics

All algorithms, statistical approaches and graphics were accomplished using MATLAB (version 9.5 R2018b), SPSS (version 25.0) and ORIGIN (version OriginPro 2017C) software, respectively. The statistical results are presented in Table 2. The P values are less than 0.001, indicating that all the extracted features are significantly different between control and HFpEF groups. HFpEF patients have a lower D/S than control as shown in Fig. 3a. For MF-DFA based features (Fig. 3b~l), the H, $h(q_{min})$, $h(q_{max})$, $\tau(q_{max})$, $\Delta\alpha$, α_{min}, α_{max} and $f(\alpha_{min})$ values of HFpEF group are lower than control group, while the $\tau(q_{min})$, $f(\alpha_{max})$ and Δf values of HFpEF group are higher. From Fig. 4, it is observed that both $h(q)$ and τ_q of control and HFpEF groups vary with q, and $f(\alpha)$ shows a single-peak bell shape.

Table 2 The statistical results of heart sound characteristics

Features	Control group	HFpEF group	*P*
D/S	1.77±0.22	1.64±0.29	<0.001
H	0.31±0.08	0.21±0.04	<0.001
$h(q_{\min})$	1.36±0.24	1.21±0.16	<0.001
$h(q_{\max})$	0.20±0.08	0.10±0.04	<0.001
$\tau(q_{\min})$	−5.07±0.72	−4.64±0.49	<0.001
$\tau(q_{\max})$	−0.39±0.24	−0.71±0.13	<0.001
$\Delta\alpha$	1.67±0.26	1.50±0.18	<0.001
$\alpha_{\min}$	−0.03±0.09	−0.15±0.05	<0.001
$\alpha_{\max}$	1.64±0.28	1.36±0.18	<0.001
$f(\alpha_{\min})$	0.30±0.07	0.27±0.06	<0.001
$f(\alpha_{\max})$	0.15±0.20	0.57±0.15	<0.001
Δf	−0.15±0.23	0.30±0.17	<0.001

The experimental result of HS classification

A dataset consisting of 12 features with significant differences was input into ELM for HFpEF identification. The classification accuracy was calculated via the four-fold cross validation. *Sigmoid* was selected as the activation function and the hidden neurons L was set as 60 according to Fig. 5. In addition, the SVM with gaussian radial basis kernel function, whose parameter values were selected by particle swarm optimization algorithm, was designed for comparison in order to verify the superiority of ELM. The performance comparison of ELM and SVM is presented in Table 3, it is noted that the ELM achieved an accuracy of 96.32%, a sensitivity of 95.48% and a specificity of 97.10%, which are 2.31%, 2.58%, and 2% higher than SVM. Moreover, the ELM shows a faster speed (nearly 1,384 times) than SVM.

Discussion

The distinctions of HS characteristics between healthy people and HFpEF patients

The D/S value can assess whether the blood perfusion time of myocardial during diastole is sufficient or not, and a higher D/S shows a healthier myocardial perfusion state [10]. The pathophysiology of HFpEF remains not completely clear yet. A preliminary consensus suggests that systemic low-grade

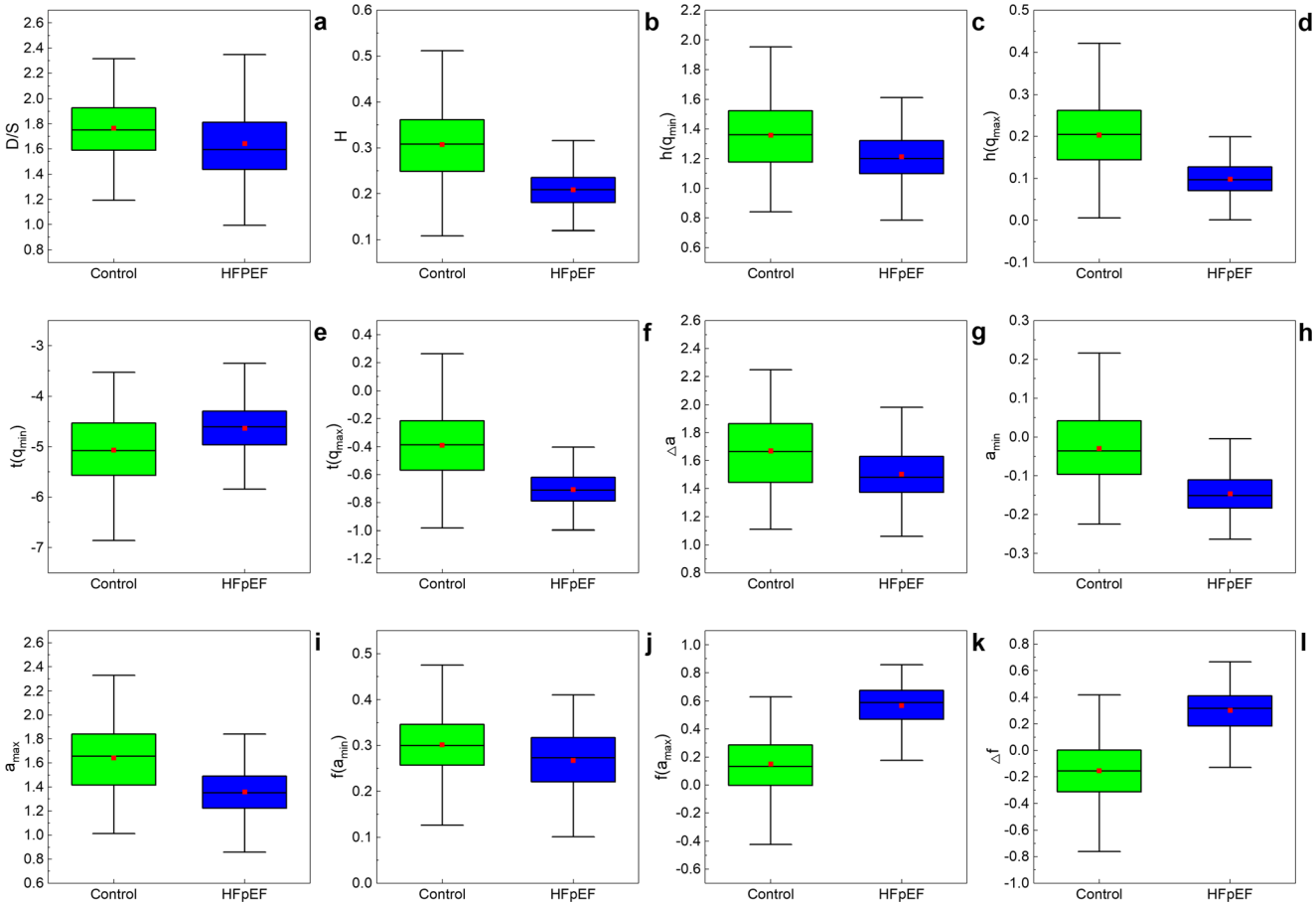

Fig. 3 The box plots showing variations of the selected features between control and HFpEF groups: **a** D/S, **b** ~ **l** MF-DFA based features, namely H, $h(q_{\min})$, $h(q_{\max})$, $\tau(q_{\min})$,$\tau(q_{\max})$, $\Delta\alpha$, $\alpha_{\min}$, $\alpha_{\max}$, $f(\alpha_{\min})$, $f(\alpha_{\max})$ and Δf

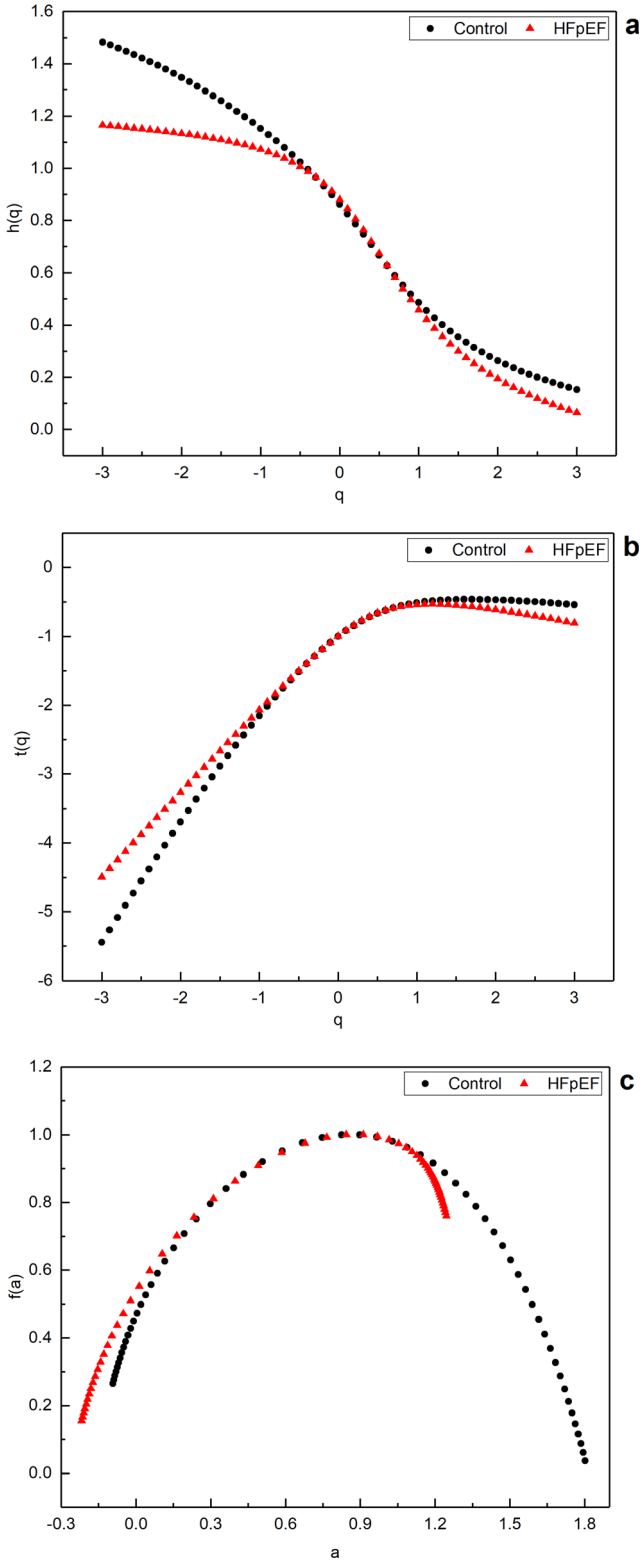

Fig. 4 The plots in MF-DFA of control and HFpEF groups: **a** plot of $h(q)$ versus q, **b** plot of $\tau(q)$ versus q, **c** plot of $f(\alpha)$ versus α

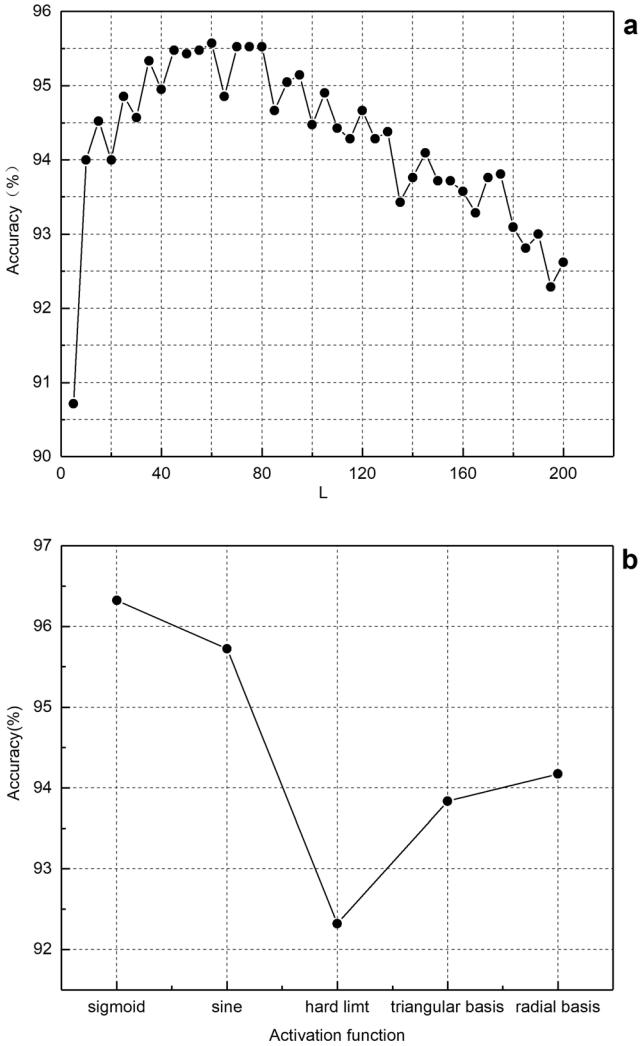

Fig. 5 The accuracy comparison of different parameters: **a** the number of hidden neurons L, **b** activation function

inflammation and microvascular dysfunction are keystones to the etiology of HFpEF [31]. Microvascular dysfunction affects peripheral vascular resistance and blood pressure, as well as (cardiac) muscle perfusion and metabolism [32]. Thus, the D/S value of HFpEF is lower, which means that the healthy people have a relatively long diastolic period and can store more nutrients and oxygen for systolic work.

Since this is the first report for analyzing and detecting HFpEF using HS, the MF-DFA based features are only used to characterize and identify HFpEF without exploring its reasons for variation. According to the multifractal theory, $0 < H < 0.5$ implies that the time series is long-range anti-correlated, and a smaller H of HFpEF indicates a stronger anti-correlation [9]. The variational generalized Hurst exponent demonstrates that the long-range correlations of large and small fluctuations are different, so that the HS of both healthy people and HFpEF patients are multifractal in nature, and a lower $\Delta\alpha$ indicates a decrease of multifractal strength of HFpEF. $h(q_{\min})$ and $h(q_{\max})$ reflect the attenuation rate of the minimum and maximum fluctuations near the position being analyzed, respectively [33], lower values of $h(q_{\min})$ and $h(q_{\max})$ show a rougher fluctuations, hence, murmurs may generate in HS signals of

Table 3 The performance comparison of different classifiers

Classifiers	Train	Test	Performance			
			Accuracy (%)	Sensitivity (%)	Specificity (%)	Time (s)
ELM	Control = 294 HFpEF = 338	Control = 107 HFpEF = 103	96.32	95.48	97.10	1
SVM	Control = 294 HFpEF = 338	Control = 107 HFpEF = 103	94.01	92.90	95.10	1,384

HFpEF patients. α_{max} and $\alpha_{\min}$ illustrate the singularity of the smallest and largest fluctuations of signal, whose intensity is inversely proportional to the value of α [34], therefore, an increase of the singularity can be obtained with the decreased α_{max} and $\alpha_{\min}$. In addition, the variation of Δf from negative to positive indicates that the multifractal spectrum of normal HS is a unimodal convex curve with a left hook-like shape, while it changed into a unimodal convex curve with a right hook-like shape for HFpEF as shown in Fig. 4c.

The advantages and limitations of the proposed method

The advantages of the method presented in this paper are reflected in three aspects. Firstly, this is the first report using HS characteristics to identify HFpEF, which is non-invasive, convenient and low-cost. Secondly, the D/S value was calculated and the information of MF-DFA was fully considered, which can not only express the differences of myocardial perfusion status, but also reflect its variations in multifractal intensity, long-range correlation and singularity etc. This is different from the studies [10, 35]. Finally, ELM was employed for HFpEF identification and achieved a better performance as well as a 1,384 times faster speed than SVM which was widely used in HS classification in previous studies [14, 36]. However, the proposed method cannot be fully verified due to the lack of globally acknowledged HS databases, and the physical meaning of $\tau(q_{\min})$ and $\tau(q_{\max})$ is not fully understood.

Conclusion

In this paper, the HS characteristics were extracted for HFpEF identification based on ELM classifier. The experimental results validate the effectiveness of the proposed method. This is also a preliminary exploration for HFpEF detection using HS characteristics, and several conclusions can be obtained as follows: (1) The myocardial perfusion status of HFpEF patients is worse than healthy people. (2) There is a loss of multifractal intensity of HS signal of HFpEF. (3) The HS of HFpEF patients shows a stronger anti-correlation than normal. (4) The singularity is increased, and the HS signal of HFpEF becomes rougher. (5) The multifractal spectrum of normal HS is a unimodal convex curve with a left hook-like shape, while it changed into a unimodal convex curve with a right hook-like shape for HFpEF.

In the future, more standard HS signals should be applied to verify the approach proposed in this paper. Moreover, the relationship between the physical significance of MF-DFA based features and the pathophysiological mechanism of HFpEF should be investigated further. The research on HFpEF is still in its infancy, and this study manifests the validity of HS for HFpEF diagnosis.

Acknowledgments This study is funded by the National Natural Science Foundation of China (No. 31570003, 31870980 and 31800823).

Compliance with ethical standards

Conflict of interest The authors declare that they have no conflict of interest.

Ethical approval All procedures performed in studies involving human participants were in accordance with the ethical standards of the institutional and/or national research committee and with the 1964 Helsinki declaration and its later amendments or comparable ethical standards.

This article does not contain any studies with animals performed by any of the authors.

Informed consent Informed consent was obtained from all individual participants included in the study.

References

1. Csp, L., Gamble, G. D., Ling, L. H. et al., Mortality associated with heart failure with preserved vs. reduced ejection fraction in a prospective international multi-ethnic cohort study. *Eur. Heart J.* 39(20): 1770–1780, 2018. https://doi.org/10.1093/eurheartj/ehy005.
2. Borlaug, B. A., and Paulus, W. J., Heart failure with preserved ejection fraction: Pathophysiology, diagnosis, and treatment. *Eur. Heart J.* 32(6):670, 2011. https://doi.org/10.1093/eurheartj/ehq426.
3. Shah, K. S., Xu, H. L., Matsouaka, R. A. et al., Heart failure with preserved, borderline, and reduced ejection fraction 5-year outcomes. *J. Am. Coll. Cardiol.* 70(20):2476–2486, 2017. https://doi.org/10.1016/j.jacc.2017.08.074.
4. Ponikowski, P., Voors, A. A., Anker, S. D. et al., 2016 ESC guidelines for the diagnosis and treatment of acute and chronic heart failure: The task force for the diagnosis and treatment of acute and chronic heart failure of the European Society of Cardiology (ESC). Developed with the special contribution of the heart failure

association (HFA) of the ESC. *Eur. J. Heart Fail.* 18(8):891–975, 2016. https://doi.org/10.1002/ejhf.592.
5. Madamanchi, C., Alhosaini, H., Sumida, A. et al., Obesity and natriuretic peptides, BNP and NT-proBNP: Mechanisms and diagnostic implications for heart failure. *Int. J. Cardiol.* 176(3):611–617, 2014. https://doi.org/10.1016/j.ijcard.2014.08.007.
6. Telles, F., and Marwick, T. H., Imaging and Management of Heart Failure and Preserved Ejection Fraction. *Curr. Treat. Options Cardiovasc. Med.* 20(11):90–90, 2018. https://doi.org/10.1007/s11936-018-0689-9.
7. Wu, C. F., Herman, B. A., Retta, S. M. et al., On the closing sounds of a mechanical heart valve. *Ann. Biomed. Eng.* 33(6):743–750, 2005. https://doi.org/10.1007/s10439-005-3237-1.
8. Gnitecki, J., Moussavi, Z., Ieee, Variance fractal dimension trajectory as a tool for heart sound localization in lung sounds recordings. In: Proceedings of the 25th Annual International Conference of the Ieee Engineering in Medicine and Biology Society, Vols 1–4: A New Beginning for Human Health, vol 25. Proceedings of Annual International Conference of the Ieee Engineering in Medicine and Biology Society. p 2420–2423, 2003.
9. Kantelhardt, J. W., Zschiegner, S. A., Koscielny-Bunde, E. et al., Multifractal detrended fluctuation analysis of nonstationary time series. *Physica A.* 316(1–4):87–114, 2002. https://doi.org/10.1016/s0378-4371(02)01383-3.
10. Zheng, Y., Guo, X., Qin, J. et al., Computer-assisted diagnosis for chronic heart failure by the analysis of their cardiac reserve and heart sound characteristics. *Comput. Methods Prog. Biomed.* 122(3):372–383, 2015. https://doi.org/10.1016/j.cmpb.2015.09.001.
11. Sikdar, D., Roy, R., and Mahadevappa, M., Epilepsy and seizure characterisation by multifractal analysis of EEG subbands. *Biomed. Signal Process. Control* 41:264–270, 2018. https://doi.org/10.1016/j.bspc.2017.12.006.
12. Lin, J., and Chen, Q., Fault diagnosis of rolling bearings based on multifractal detrended fluctuation analysis and Mahalanobis distance criterion. *MSSP* 38(2):515–533, 2013. https://doi.org/10.1016/j.ymssp.2012.12.014.
13. Tang, J., Wang, D., Fan, L. et al., Feature parameters extraction of GIS partial discharge signal with multifractal Detrended fluctuation analysis. *ITDEI* 22(5):3037–3045, 2015. https://doi.org/10.1109/tdei.2015.004556.
14. Zheng, Y., Guo, X., and Ding, X., A novel hybrid energy fraction and entropy-based approach for systolic heart murmurs identification. *Expert Syst. Appl.* 42(5):2710–2721, 2015. https://doi.org/10.1016/j.eswa.2014.10.051.
15. Lin, S.-W., Ying, K.-C., Chen, S.-C. et al., Particle swarm optimization for parameter determination and feature selection of support vector machines. *Expert Syst. Appl.* 35(4):1817–1824, 2008. https://doi.org/10.1016/j.eswa.2007.08.088.
16. Zhang, X., Chen, X., and He, Z., An ACO-based algorithm for parameter optimization of support vector machines. *Expert Syst. Appl.* 37(9):6618–6628, 2010. https://doi.org/10.1016/j.eswa.2010.03.067.
17. Zhang, Y., and Zhang, P., Machine training and parameter settings with social emotional optimization algorithm for support vector machine. *Pattern Recogn. Lett.* 54:36–42, 2015. https://doi.org/10.1016/j.patrec.2014.11.011.
18. Huang, G.-B., Zhu, Q.-Y., and Siew, C.-K., Extreme learning machine: Theory and applications. *Neurocomputing* 70(1–3):489–501, 2006. https://doi.org/10.1016/j.neucom.2005.12.126.
19. Huang, G.-B., Zhou, H., Ding, X. et al., Extreme learning machine for regression and multiclass classification. *IEEE Trans Syst Man Cybern B Cybern* 42(2):513–529, 2012. https://doi.org/10.1109/tsmcb.2011.2168604.
20. Debbal, S. M., and Bereksi-Reguig, F., Time-frequency analysis of the first and the second heartbeat sounds. *Appl. Math. Comput.* 184(2):1041–1052, 2007. https://doi.org/10.1016/j.amc.2006.07.005.
21. Omari, T., and Bereksi-Reguig, F., An automatic wavelet denoising scheme for heart sounds. *Int. J. Wavelets Multiresolution Inf. Process.* 13(3), 2015. https://doi.org/10.1142/s0219691315500162.
22. Liang, J., Zhao, J., and Hao, Y., An image denoising and enhancement algorithm for inner and outer ring of wavelet bearings based on improved threshold. In: Tseng, J., Kotenko, I., (Eds.), 3rd Annual International Conference on Information System and Artificial Intelligence, vol 1069. *J. Phys. Conf. Ser.* 2018. https://doi.org/10.1088/1742-6596/1069/1/012158
23. Jain, P. K., and Tiwari, A. K., An adaptive thresholding method for the wavelet based denoising of phonocardiogram signal. *Biomed. Signal Process. Control* 38:388–399, 2017. https://doi.org/10.1016/j.bspc.2017.07.002.
24. Chourasia, V. S., Tiwari, A. K., and Gangopadhyay, R., A novel approach for phonocardiographic signals processing to make possible fetal heart rate evaluations. *DSP* 30:165–183, 2014. https://doi.org/10.1016/j.dsp.2014.03.009.
25. Xiao, S. Z., Guo, X. M., Wang, F. L. et al., Evaluating two new indicators of cardiac reserve. *IEEE Eng. Med. Biol. Mag.* 22(4):147–152, 2003. https://doi.org/10.1109/memb.2003.1237516.
26. Springer, D. B., Tarassenko, L., and Clifford, G. D., Logistic regression-HSMM-based heart sound segmentation. *IEEE Trans. Biomed. Eng.* 63(4):822–832, 2016. https://doi.org/10.1109/tbme.2015.2475278.
27. Liu, C., Springer, D., and Clifford, G. D., Performance of an open-source heart sound segmentation algorithm on eight independent databases. *Physiol. Meas.* 38(8):1730–1745, 2017. https://doi.org/10.1088/1361-6579/aa6e9f.
28. Goldberger, A. L., Amaral, L. A. N., Glass, L. et al., PhysioBank, PhysioToolkit, and PhysioNet - components of a new research resource for complex physiologic signals. *Circulation* 101(23):E215–E220, 2000. https://doi.org/10.1161/01.CIR.101.23.e215.
29. Shang, P., Lu, Y., and Kamae, S., Detecting long-range correlations of traffic time series with multifractal detrended fluctuation analysis. *Chaos, Solitons Fractals* 36(1):82–90, 2008. https://doi.org/10.1016/j.chaos.2006.06.019.
30. Ihlen, E. A. F., Introduction to multifractal detrended fluctuation analysis in Matlab. *Front. Physiol.* 3, 2012. https://doi.org/10.3389/fphys.2012.00141.
31. Rech, M., Aizpurua, A. B., van Empel, V. et al., Pathophysiological understanding of HFpEF: microRNAs as part of the puzzle. *Cardiovasc. Res.* 114(6):782–793, 2018. https://doi.org/10.1093/cvr/cvy049.
32. Serne, E. H., de Jongh, R. T., Eringa, E. C. et al., Microvascular dysfunction a potential pathophysiological role in the metabolic syndrome. *Hypertension* 50(1):204–211, 2007. https://doi.org/10.1161/hypertensionaha.107.089680.
33. Shang, P., Lu, Y., and Kama, S., The application of holder exponent to traffic congestion warning. *Physica A.* 370(2):769–776, 2006. https://doi.org/10.1016/j.physa.2006.02.032.
34. Chattopadhyay, A., Khondekar, M. H., and Bhattacharjee, A. K., Fractality and singularity in CME linear speed signal: Cycle 23. *Chaos, Solitons Fractals* 114:542–550, 2018. https://doi.org/10.1016/j.chaos.2018.08.008.
35. Azmy, M. M., Mohamady, R., Heart sounds recognition using multifractal detrended fluctuation analysis and support vector machine. In: AlOqily, I., (Ed.), 2017 Ieee Jordan Conference on Applied Electrical Engineering and Computing Technologies. IEEE Jordan Conference on Applied Electrical Engineering and Computing Technologies. 2017.
36. Choi, S., Detection of valvular heart disorders using wavelet packet decomposition and support vector machine. *Expert Syst. Appl.* 35(4):1679–1687, 2008. https://doi.org/10.1016/j.eswa.2007.08.078.